Probing transient protein-mediated DNA linkages using nanoconfinement

Maedeh Roushan, Parminder Kaur, Alena Karpusenko, Preston J. Countryman, Carlos P. Ortiz, Shuang Fang Lim, Hong Wang, and Robert Riehn

Citation: Biomicrofluidics **8**, 034113 (2014); doi: 10.1063/1.4882775
View online: http://dx.doi.org/10.1063/1.4882775
View Table of Contents: http://scitation.aip.org/content/aip/journal/bmf/8/3?ver=pdfcov
Published by the AIP Publishing

Probing transient protein-mediated DNA linkages using nanoconfinement

Maedeh Roushan, Parminder Kaur, Alena Karpusenko, Preston J. Countryman, Carlos P. Ortiz, Shuang Fang Lim, Hong Wang, and Robert Riehn[a)]
Department of Physics, NC State University, Raleigh, North Carolina 27695, USA

(Received 18 April 2014; accepted 30 May 2014; published online 12 June 2014)

We present an analytic technique for probing protein-catalyzed transient DNA loops that is based on nanofluidic channels. In these nanochannels, DNA is forced in a linear configuration that makes loops appear as folds whose size can easily be quantified. Using this technique, we study the interaction between T4 DNA ligase and DNA. We find that T4 DNA ligase binding changes the physical characteristics of the DNA polymer, in particular persistence length and effective width. We find that the rate of DNA fold unrolling is significantly reduced when T4 DNA ligase and ATP are applied to bare DNA. Together with evidence of T4 DNA ligase bridging two different segments of DNA based on AFM imaging, we thus conclude that ligase can transiently stabilize folded DNA configurations by coordinating genetically distant DNA stretches. © *2014 AIP Publishing LLC*.
[http://dx.doi.org/10.1063/1.4882775]

I. INTRODUCTION

Protein-mediated DNA loops play a central role in many biological processes.[1,2] DNA looping is involved in transcription,[3] repair,[4] telomere maintenance,[5] and gene regulation.[6] In general, protein-mediated DNA looping enables DNA regions separated by a large genetic distance to interact with each other. The formation of very large loops (10s to 100s of kbp) in the emergence of chromatin organization and the necessity of this chromatin organization for normal cell function is an intensive focus of recent research.[7–9] In particular, the co-operative action of multiple protein copies in promoting DNA looping[10–13] and conformational change[14] has become a central question. Here we demonstrate a tool for detecting transient interactions that may be important in facilitating looping transitions (Fig. 1).

The most established method for quantifying DNA loop formation is the gel electrophoresis mobility shift assay.[15] Protein-mediated DNA loops can also be directly visualized by atomic force microscopy (AFM) or transmission electron microscopy (TEM).[3–5] These single-molecule techniques have the advantage of detecting rare states. However, only configurations of DNA molecules smaller than 10 kbp in length can be easily interpreted if molecules are randomly deposited on a surface from solution. DNA bending and looping on a even shorter scale (10s of bp) can be detected by fluorescence energy transfer, and important information about the single-molecule dynamics can be established.[16,17] Tethered particle motion (TPM) is also able to monitor the temporal fluctuation of DNA, but does so on a larger scale.[18–20] However, similar to force-based measurements, it requires the modification of the DNA ends.[21–23] That potentially limits the utility for studying proteins that not only catalyze internal loops, but also end-to-end circularization. In principle, optical microscopy can follow the temporal course of loop formation,[24] but in general it requires resolution enhancement techniques to follow loops in the range of a few kbp, which in turn lower the temporal resolution.[25] Stretching DNA in flow cells

[a)]RRiehn@ncsu.edu

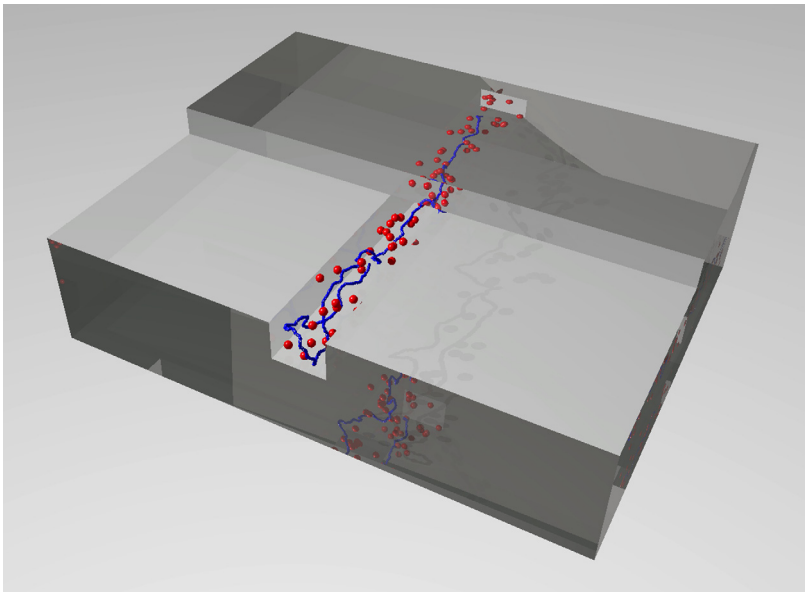

FIG. 1. Schematic of nanochannel-stretched DNA (blue) with weakly-binding protein particles (red). Proteins are larger than actual for easy visibility. In the foreground, there is a folded DNA configuration.

overcomes the resolution problem, but notably the extending stress is very heterogeneous along the molecule making a quantitative evaluation difficult.[26]

We will use stretching of DNA in nanochannels as the main analytic technique for following DNA loop configurations in this publication.[27] Such nanochannels have a cross-section of $\sim$100 $\times$ 100 nm^2, and a length of 100 μm. After DNA is brought into a nanochannel, it will assume an equilibrium configuration that is governed by the channel cross-section, the contour length of DNA, its persistence length, and its width.[28] The dependence on the persistence length and width make nanochannel stretching a promising probe for these parameters as a function of buffer conditions[29] or protein binding.[30–32] DNA is dynamic inside nanochannels and fluctuates,[33–35] and can thus explore many possible configurations during a single experiment. Furthermore, the configuration of looped[36] and knotted[37] molecules can be followed in real time (Fig. 1).

Cyclization by T4 DNA ligase is an intensively studied model system for DNA looping.[38–41] T4 DNA ligase displays a surprisingly large range of functionalities. T4 DNA ligase catalyzes formation of the phosphodiester bond between the adjacent 5′-PO_4 and 3′-OH groups at DNA ends of double-stranded DNA (dsDNA) fragments.[42] It joins dsDNA in both blunt-ended ligation and the ligation of complimentary ends, which is the same as nick ligation. It also ligates single-stranded DNA (ssDNA), albeit with very low efficiency,[43] seals single-stranded 1–5-nucleotide gaps,[44] and acts as a lyase by removing apurininc/apyrimidinic (AP) sites.[45] T4 DNA ligase requires the co-factors adenosine triphosphate (ATP) and Mg^{2+} for full activity. ATP is required for specific binding of ligase to both DNA strands, while Mg^{2+} is required for catalytic action.[46,47] At high T4 DNA ligase concentration, non-specific binding to dsDNA was observed. Furthermore, it was proposed that the apparent persistence length of DNA drops in presence of a high concentration T4 DNA ligase,[48,49] which is likely due to ligase induced DNA kinking and local base-pair opening in transient DNA-ligase complexes.[50]

In studies that focus on the mechanical properties of DNA, T4 DNA ligase is typically used at a low concentration to secure circular configurations that are at formed through hybridization of complimentary ends.[38] Thus, the cyclization rate is governed by the probability of a both ends coming together, specifically as a function of DNA length, DNA stiffness, and swelling of the coil.[38,40,51] While the self-interaction probability of relaxed yeast chromatin indicates the validity of the worm-like chain model,[52] we note that ligase-based looping seems more efficient than predicted by that model for larger distances (>1 kbp).[40]

We can speculate on the connection between the efficient formation of very large loops (>1 kbp) and both blunt-ended dsDNA and ssDNA ligation capability. In order to ligate distinct DNA molecules, the enzyme has to bind to two DNA molecules simultaneously and locate their ends. That means three entities (1st end, 2nd end, ligase or ligase multimer) have to come together in a small volume. In analogy with search process of transcription factors and other sequence-specific enzymes, we speculate that the DNA looping rate is enhanced through a facilitated diffusion process in which the protein first binds to a nonspecific motif, and then translocates along the strand to locate DNA ends.[53] We will show evidence that non-specific DNA-protein-DNA clusters are formed even at internal DNA-DNA junctions.

In this publication, we investigate the influence of T4 DNA ligase and its cofactor ATP on the configuration of long DNA strands under nanoconfinement. Under the Mg^{2+}-free conditions chosen by us, ligase is not capable of covalent strand-joining and is known to bind DNA independent of its catalytic action. We introduced λ-DNA molecules into nanochannels and observed extended and folded DNA configurations (Figs. 1 and 2). We observed a contraction of DNA in presence of T4 DNA ligase. We further recorded a strongly increased probability of folded DNA configurations in presence of T4 DNA ligase. These folded configurations gradually unfolded, and we observed that the rate of DNA unfolding reduced under ATP exposure. We attribute this slowing of unfolding to the establishment of transient, T4 DNA ligase-mediated DNA-DNA links. AFM imaging supports the hypothesized notion that transient DNA-DNA contacts are stabilized by T4 DNA ligase. We speculate that such transient stabilization of DNA-DNA contacts may be a general mechanism to increase the rate of protein-induced DNA looping.

II. EXPERIMENTAL

λ-DNA (Roche Diagnostics GmbH) was stained with YOYO-1 (Life Sciences) at a ratio of 1 dye per 10 base pairs. The contour length of unstained λ-DNA (48.5 kbp) is approximately 16 μm. After staining, that length can increase by up to 30%.[54] DNA was suspended in 0.5 × TBE buffer (pH 8) at room temperature. BSA (0.1 mg/ml, New England Biolabs) was added to prevent sticking of DNA to the nanochannels. For experiments requiring ATP, the final ATP concentration was 1 mM.

We chose T4 DNA ligase supplied by Roche Diagnostics (1 $U_{Roche}/\mu l$), since this vendor does not supplement their product with BSA. The latter would interfere with the interpretation of our AFM measurements. The T4 DNA ligase stock solution was expected to have a

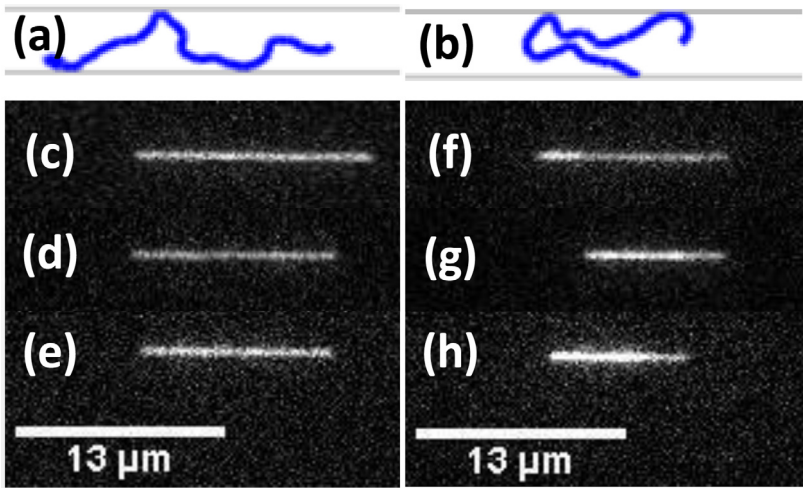

FIG. 2. Observed configurations of λ-DNA molecules in nanochannels. (a) and (b) are schematics of extended and folded structures, respectively. (c)-(e) are fluorescence micrographs of extended configurations and are (f)-(h) fluorescence micrographs of folded configurations. (c) and (f) are bare λ-DNA, (d) and (g) are λ-DNA with T4 DNA ligase, and (e) and (h) are λ-DNA with T4 DNA ligase and ATP.

concentration of 6 μM, while we measured a concentration of 10.4 μM via absorption spectroscopy. We also observed that T4 DNA ligase is predominantly in a multimeric state using dynamics light scattering (DLS), with some large aggregates, possibly due to the fact that this vendor does not add BSA. We thus believe the concentration of *active* T4 DNA ligase molecules is considerably lower. Using Roches units, the final T4 DNA ligase concentration is 5 U_{Roche}/ml.

The majority of recent publications in the field use T4 DNA ligase supplied by New England Biolabs, which contains BSA. Using the same unit definition as New England Biolabs, the final concentration of T4 DNA ligase is in the range of 500 U_{NEB}/ml to 1000 U_{NEB}/ml (1 U_{NEB}/ml = 0.02 nM (Ref. 50)). This compares to 250 U_{NEB}/ml used by Widom and Cloutier,[48,55] 1 U_{NEB}/ml used by low-concentration studies such as Du *et al.*,[49] and a few 10^4 U_{NEB}/ml by Yuan *et al.*[50] We verified that nanochannel measurements with an equivalent concentration of T4 DNA ligase from both New England Biolabs and Roche gave similar results.

Samples were prepared in the following sequence: DNA was suspended in buffer at 1 μg/ml and heated to 65 °C for 10 min before being rapidly cooled on ice. BSA was added. T4 DNA ligase and ATP were added as necessary, and the sample was incubated for 15 min at room temperature. Then a 100 mM YOYO-1 stock solution was added, and the solution was incubated for four hours at 4 °C. The solution was briefly spun down in a microcentrifuge prior to experiments.

All experiments used mixed micro- and nano-fluidic devices made from fused silica, which were prepared by methods discussed elsewhere.[56] Nanofluidic channels with a 50×100 nm^2 cross-section and a length of 200 μm were placed between u-shaped microchannels that were 100 μm wide, 800 nm deep, and had about 1 cm separation between inlets and active zone.[57] Each DNA molecule is driven from microchannel to nanochannel by a hydrostatic pressure gradient. After the DNA molecule has entered the nanochannel, the pressure gradient is removed and the dynamics of molecules are observed. Molecules were observed using an inverted fluorescence microscope with a 1.3-N.A. oil-immersion microscope objective (Nikon, TE-2000) under illumination from a metal halide lamp, and observation by an emCCD camera (Andor).

We followed the conventional approach of representing the brightness of a stretched DNA molecule as the convolution of a boxcar function and a Gaussian.[27] However, since a brightness step within the molecule is present for folded molecules, two such functions are necessary. For calculating the end-to-end and the loop length of DNA molecules, we fitted the brightness along the molecule backbone to

$$I(x) = I_b + \frac{I_f - I_u}{2}\left(\mathrm{erf}\left(\frac{x - x_f + \frac{l_f}{2}}{\sigma}\right) - \mathrm{erf}\left(\frac{x - x_f - \frac{l_f}{2}}{\sigma}\right)\right) + \frac{I_u}{2}\left(\mathrm{erf}\left(\frac{x - x_u + \frac{l_u}{2}}{\sigma}\right) - \mathrm{erf}\left(\frac{x - x_u - \frac{l_u}{2}}{\sigma}\right)\right), \quad (1)$$

where $I(x)$ is the intensity along nanochannel, σ is the slope of the edge, I_u, and I_f are the brightnesses of the unfolded and folded sections. x_u and l_u are the center and length of the entire molecule. x_f and l_f are the center and length of the folded stretch. I_b is a constant background term.

For AFM imaging, we diluted linear DNA (3.8 kbps) in AFM deposition buffer (25 mM HEPES, 25 mM Sodium Acetate, pH 7.5). The final DNA concentration was 1 ng/μl for all measurements. For measurements with T4 DNA ligase and ATP, the respective final concentrations were 5 U_{Roche}/ml (Roche) and 1 mM, respectively. Solutions were incubated at room temperature for 15 min. APTES mica surfaces were prepared as described earlier.[58] A droplet of the DNA or T4 DNA ligase-DNA-ATP solution was added onto an APTES treated mica surface and incubated for 30 min. Surfaces were further washed with deionized water and dried with dry nitrogen. Imaging was performed in non-contact mode in air (cantilevers: Nanosensors, PPPFMR; resonant frequency: ~45-115 kHz, spring constant: 0.5–9.5 N/m) using an Asylum MFP3D AFM instrument.

III. RESULTS

Upon introduction of λ-DNA into nanochannels, we observed two predominant configurations (Fig. 2). The *extended configuration* (Fig. 2(a)) is characterized by constant fluorescence intensity along the channel (Figs. 2(b)–2(d)). In the *folded configuration* (Fig. 2(e)), a hairpin causes the molecule to fold back on itself. A step in the molecule brightness can be observed (Figs. 2(f)–2(h)). DNA molecules entered the nanochannel randomly in either an unfolded or folded configurations. The folded configurations are not simply density fluctuations of extended molecules.[34,35] In particular, the bright region of a fold is always linked to one end, and the onset within the molecule is sudden. In contrast, thermal density fluctuations of an extended molecule are well described by Rouse modes. Their phase is in general random, so that they do not form stable step-like configurations. After observation effects are taken into account, these fluctuations also cannot reach the intensity magnitude found here.

We analyzed the intensity profiles of extended λ-DNA molecules, and found the mean end-to-end lengths by fitting to Eq. (1) after applying the constraint $I_f = I_u$. The histogram in Fig. 3 shows the distribution of end-to-end of lengths of extended DNA molecules for the three different datasets. A Gaussian is fit to each distribution to obtain the mean end-to-end lengths, listed in Table I. We find that λ-DNA contracted in the presence of T4 DNA ligase, from 14.4 μm for bare DNA to 12.5 μm with T4 DNA ligase. We attribute the further contraction and narrowing of the distribution upon addition of ATP mainly to an interference of the dye with ATP, and not an actual effect of ATP (separate manuscript in preparation). We have found no evidence that the increase of the ionic strength from $\sim$15 mM lowers the extension strongly if DAPI is used for DNA visualization. Reisner reported such a reduction as funciton of ionic strength.[29]

DNA configurations are dynamic, and we followed molecules for at least 30 s. Folded molecules under all conditions gradually unroll until molecules reach an extended configuration, as reported by Levy.[36] We show intensity time traces of the recoil process in (Figs. 4(a)–4(c)). We quantified the configuration parameters by fitting the full form of Eq. (1) to intensity profile of along the nanochannel (Figs. 4(d)–4(f)). The unrolling process occurs over 10s of seconds, and is considerably slower than the relaxation time of both density fluctuations[34,35] and the connected relaxation of length fluctuations[33,35] that occur within a few seconds. Thus, we feel further strengthened in applying Levy's loop interpretation.[36]

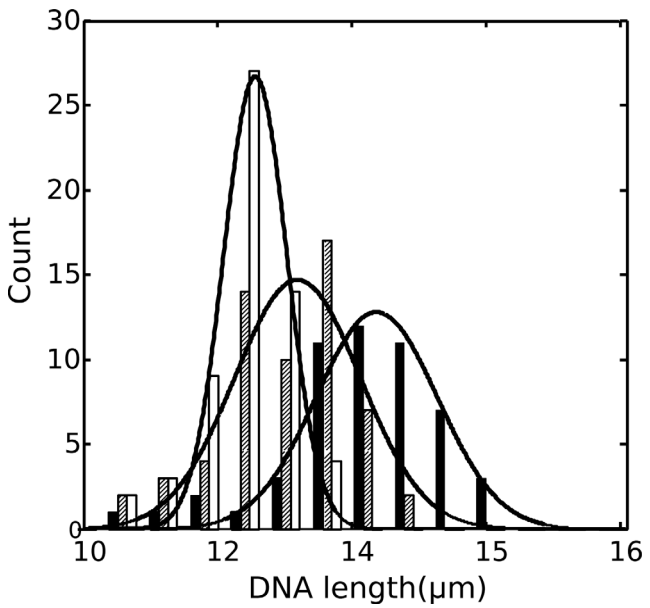

FIG. 3. Histogram of end-to-end lengths of extended DNA molecules, bare λ-DNA (solid bars), λ-DNA with T4 DNA ligase (gray bars), and λ-DNA with T4 DNA ligase and ATP (white bars). A Gaussian was fit to each distribution to determine the mean end-to-end DNA lengths (see Table I).

TABLE I. Statistical characterization of DNA configurations in the presence of T4 DNA ligase and ATP. 60 extended molecules for each condition were used to find l_u (extension of a fully unfolded molecule), Δl_u^2 (mean fluctuation amplitude of fully unfolded molecules), and K (spring constant derived from the former two quantities, see discussion). 22 folded molecules for each condition were used to find γ (ratio of apparent extensions of folded and unfolded regions). The relative product of persistence length and molecule width, Pw, was found from the mean values of l_u and γ. The probability of entry in a looped configuration, p_{loop}, was found from 100 molecules for each condition. Parameter definitions are given in the discussion.

Sample	l_u (μm)	Δl_u^2 (μm^2)	K (10^{-2} N/m)	γ	Pw (rel.)	p_{loop}
Bare λ-DNA	14.4 ± 0.1	0.218 ± 0.02	1.9 ± 0.2	1.26 ± 0.15	1.00	0.27
λ-DNA + T4 ligase	13.2 ± 0.1	0.233 ± 0.01	1.8 ± 0.1	1.10 ± 0.02	0.51 ± 0.23	0.41
λ-DNA + T4 ligase + ATP	12.5 ± 0.1	0.223 ± 0.02	1.9 ± 0.2	1.06 ± 0.02	0.39 ± 0.18	0.43

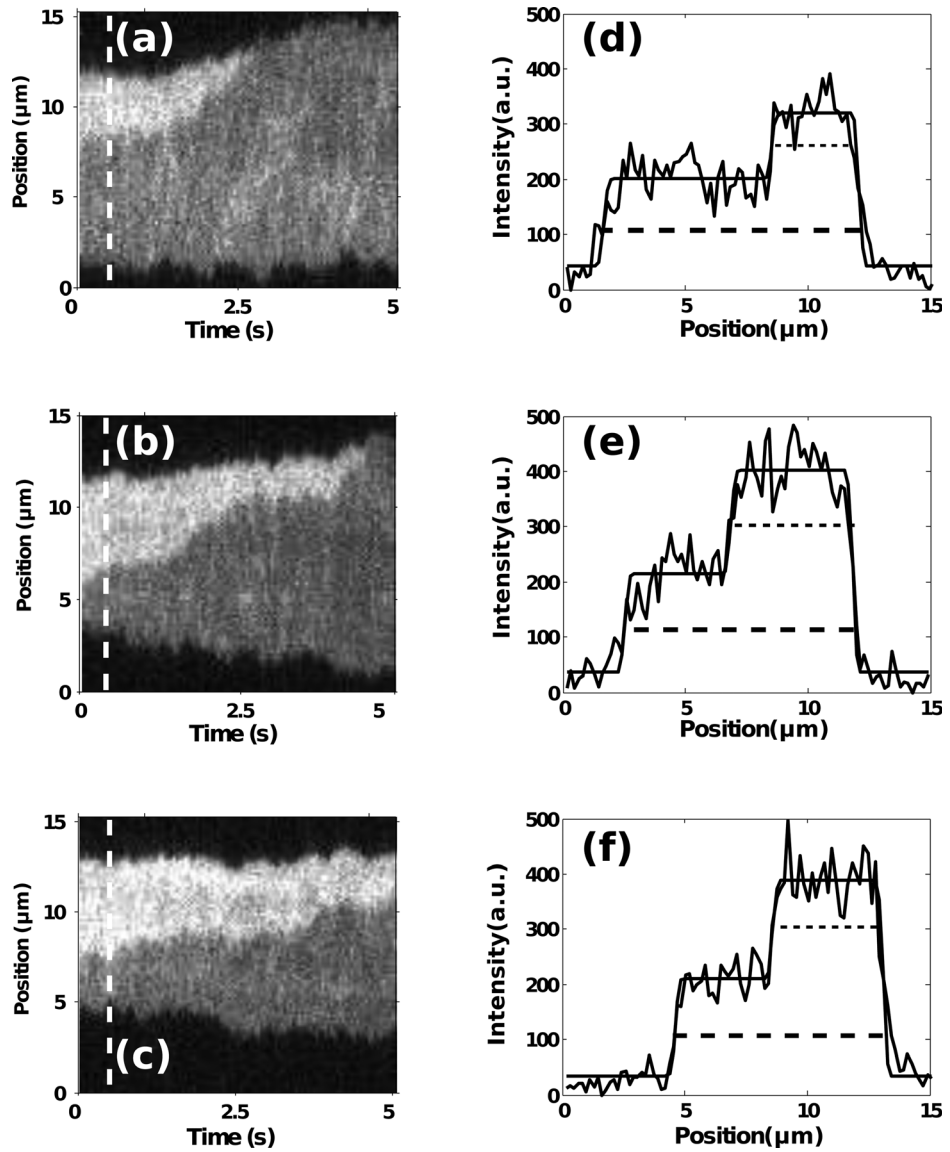

FIG. 4. Folded λ-DNA molecules in nanochannels. (a)-(c) show kymographs of fluorescence intensity along channel axis as a function of time. (d)-(f) illustrate the projected intensity of λ-DNA molecules as a function of position along the nanochannel at 0.5 s. The end-to-end DNA length of molecules is shown with dashed line and folded length is shown with dotted lines. (a) and (d) are bare λ-DNA, (b) and (e) are λ-DNA with T4 DNA ligase, and (c) and (f) are λ-DNA with T4 DNA ligase and ATP.

In order to quantify the speed of unrolling, we aligned molecules under equal conditions by shifting the time axis until curves overlapped. The resulting graphs of average loop length versus time are shown in Fig. 5. We found that loops unfold with an approximately constant rate of 216 ± 5 nm/s, 204 ± 5 nm/s, and 119 ± 3 nm/s for λ-DNA, λ-DNA with T4 DNA ligase, and λ-DNA with T4 DNA ligase and ATP, respectively (ATP alone without ligase was similar to bare DNA).

To further investigate whether or not DNA ligase directly promotes DNA looping, we performed AFM imaging on DNA deposited from a solution containing bare DNA (Fig. 6(a)), and a solution containing DNA, T4 DNA ligase and ATP (Figs. 6(b) and 6(c)). Because of the length of the chosen DNA substrate ($\sim 1.2\,\mu$m), we anticipate that the majority of DNA molecules form random DNA-DNA crossings that are an effect of the deposition of the 3-dimensional molecule to the 2-dimensional surface. Visual inspection of DNA-DNA crossings reveals that intersections in the presence of both T4 DNA ligase and ATP appear on average taller than those without (compare Fig. 6(a) to Figs. 6(b) and 6(c)).

Along the extended DNA on the surface (away from crossings), we observed a larger variability of height of the fiber in the presence of T4 DNA ligase and ATP. In particular taller sections occurred in stretches along the molecule. We attribute this to the binding of T4 DNA ligase to DNA.

We analyzed the peak height of DNA-DNA crossings in the absence or presence of DNA ligase, and observed dramatic differences (Fig. 7). In the case of bare DNA (Fig. 7(a)), a single peak is observed (0.70 ± 0.08 nm), while the histogram for DNA with T4 DNA ligase and ATP (Fig. 7(b)) showed two peaks (0.73 ± 0.05 and 1.07 ± 0.15 nm). The stated uncertainties are the half-widths of the Gaussian fits; the confidence for the peak positions is higher. The lower peak in the presence of DNA ligase (Fig. 7(b)) is consistent with the height for DNA-DNA crossing with bare DNA (Fig. 7(a)). The second peak in Fig. 7(b) corresponds to the binding of T4 DNA ligase since it is absent without DNA ligase (Fig. 7(a)). The area under the two Gaussian peaks indicates that $\sim 3/4$ of all DNA-DNA junctions are bound by ligase molecules. We are not able to distinguish whether these are monomers or multimers. That ratio matches the fraction of junctions with greater height that we visually estimated in Fig. 6.

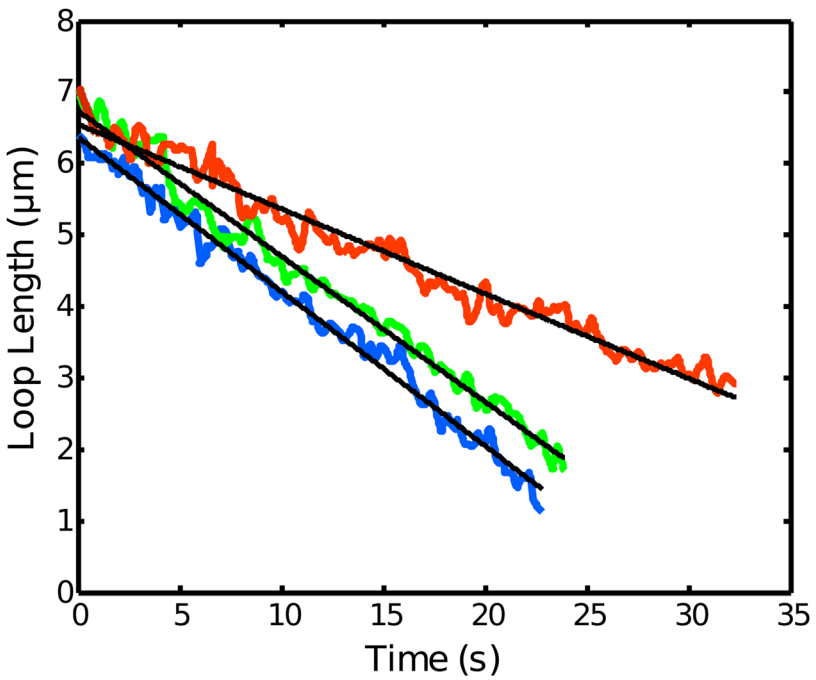

FIG. 5. Mean aligned DNA molecule loop lengths as function of time for 22 molecules per dataset with their linear fits. Bare λ-DNA (blue), λ-DNA with T4 DNA ligase (green), and λ-DNA with T4 DNA ligase and ATP (red).

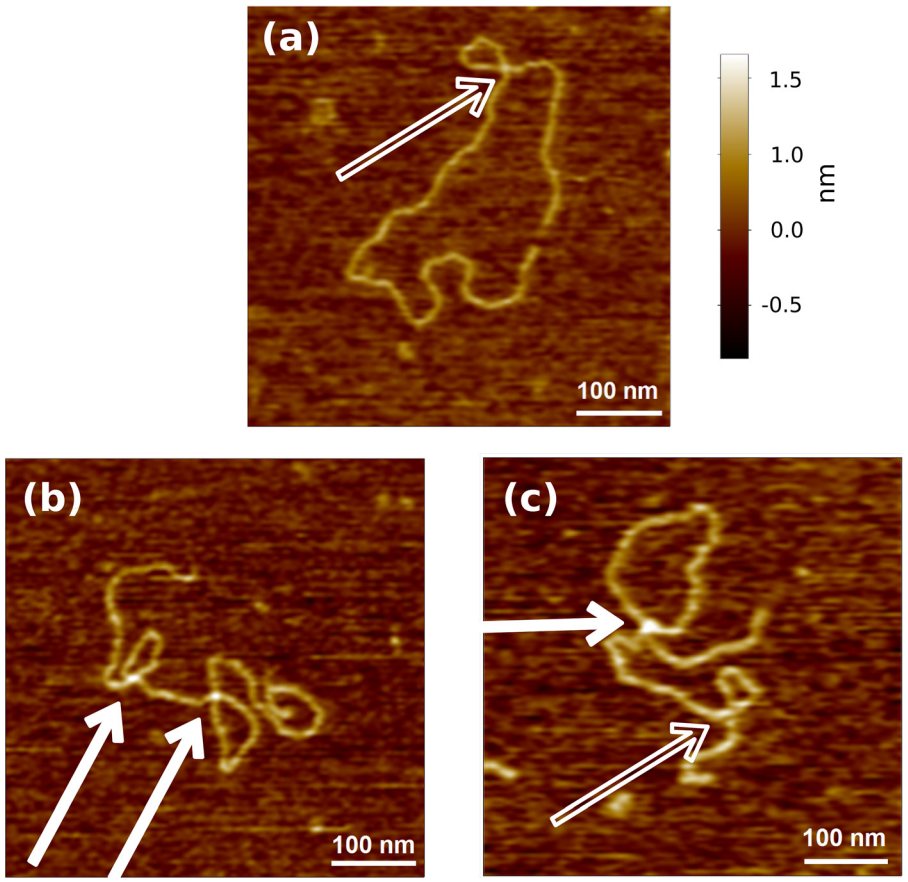

FIG. 6. AFM images of DNA-DNA crossings. (a) Bare DNA (3.8 kbp). (b) and (c) DNA with T4 DNA ligase and ATP. Solid arrows indicate higher crossings consistent with ligase binding, outlined arrows indicate shallower crossings consistent with bare DNA.

IV. DISCUSSION

It is apparent that the addition of T4 DNA ligase and the further addition of ATP modify the behavior of DNA significantly. In order to interpret the measurements, we will have to discuss them in the framework of confined polymers.

Although the theory of DNA extension under 1-d confinement is still an active field of research,[28,59] a good experimental understanding exists.[33,60] Broadly, the extension of confined DNA molecules results from a balance between entropy and excluded volume interactions within the DNA.[61] A DNA molecule of contour length L, width w, and persistence length P that is confined to a nanochannel of width D will elongate due to excluded volume interaction between segments of the polymer that are separated in genetic position along the backbone. The de Gennes theory predicts an extension l that scales as[61,62]

$$l \cong L\left(\frac{wP}{D^2}\right)^{1/3}. \tag{2}$$

However, experimental tests have shown that the scaling in D is stronger than indicated.[33] Recently, the importance of a minimum scale for self-avoidance[63] and the alignment of polymer segments[64] have been demonstrated. Interestingly, the ideal scaling of Eq. (2) is recovered for circular DNA.[60] We thus anticipate that the dependence of l on P is higher than that on w in channels with a width of 100 nm, with an exact functional relationship not clear for the extended configuration.

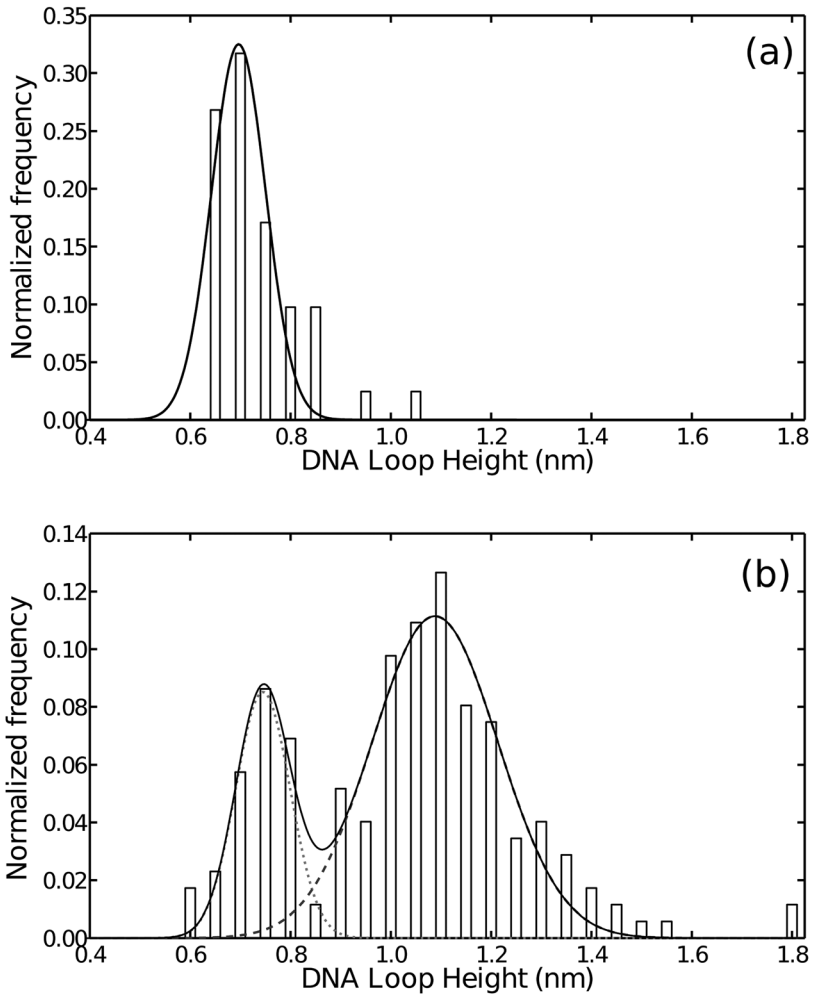

FIG. 7. Histograms of heights of DNA-DNA crossings. (a) Bare DNA (N = 41). (b) DNA with T4 DNA ligase and ATP (N = 174). The red dotted line corresponds to unoccupied crossings, the blue dashed line to occupied crossings, and the solid line is the sum of both.

There are two distinct mechanisms that can lead to an apparent shortening of DNA in nanochannels upon protein binding. The first mechanism is the formation of stable compacted DNA configurations that change the effective available contour length of the DNA. Examples include the binding of histones[30] or nucleoproteins.[31] The second mechanism is the modification of p and w, which leads to more dramatic effects under nanoconfinement than in free solution.[29,32] Decreasing l in identical channels could be the effect of a change of w or P. Neither mechanism are related to the osmotic pressure effects that can collapse DNA which occurs at higher concentration of proteins than considered here.[65–67]

To the first approximation, the effective spring constant K of unfolded molecules can be found from the fluctuation amplitude through $K = k_B T/\langle \Delta l_u^2 \rangle$,[33] where k_B is the Boltzmann constant and T is the temperature. If the scaling of Eq. (1) is combined with the free energy of deformation of the deGennes model such as given by Jun *et al.*,[68] one can predict that the spring constant is invariant under changes in (Pw) as long as the contour length is conserved. Refinements to the determination of the length fluctuation amplitude that take the measurement process and all Rouse modes into account[35] do not change this result as it applies to all modes independently. We tested whether the reduction in l was connected to a change of w and P or to a more fundamental change in molecule configuration by determining the effective spring

constant witnessed by the fluctuation amplitude in l (Table I). Addition of T4 DNA ligase to DNA as well as further addition of ATP did not change the spring constant significantly. We thus believe that all extended configurations are essentially wormlike chains of similar contour length, and that no permanent links between genetically distant loci are established.

We define α as the extension factor (length of occupied channel segment divided by contour length) of an unfolded segment of DNA. β is the extension factor of a folded segment (two times length of occupied channel segment divided by contour length). Interestingly, we can determine $\gamma = \beta/\alpha$ alternatively from the ratio of brightness's $\gamma = 2 \cdot I_u/I_f$. The γ-factor is a demonstration of the excluded volume effect, since an ideal chain should show $\gamma = 1$. Levy *et al.* reported $\gamma = 1.3$ in a configuration similar to ours.[36] We find a similar γ for bare DNA (Table I), but a strong reduction once T4 DNA ligase is introduced, and a further reduction upon ATP addition. Since the relative magnitudes of both α and γ are experimentally accessible, we can find β. Since the scaling predicted by de Gennes holds for folded segments,[60] we can assume that Eq. (2) holds and determine the product wP. We find that it is reduced to 50% upon addition of T4 DNA ligase and to 40% in the presence of ATP. This is a remarkable reduction. We are however not able to measure w and P independently, even though detailed numerical studies exist.[59,69]

Levy *et al.* have described a model for the unfolding of the folded geometry that utilizes a constant driving force due to excluded volume interaction and a drag force dominated by the drag between channel walls and DNA.[36] In the framework of this model, the decreased unfolding rate in the presence of T4 DNA ligase and ATP could be interpreted as a reduction of the effective width of the chain. The looping und unfolding process in nanochannels has numerically been treated by Cifra and Bleha,[70] but for relatively short chains and without hydrodynamic interactions. Račko and Cifra[71] have treated kinetics of the segregation two independent chains in nanochannels, which is interesting, but topologically different. A recent study by Chen did note that some folded molecules can become trapped in a folded state for extended times.[72]

We have found two potential problems with Levy's model.[36] First, the model is missing a force term for $\gamma > 1$. We have modified the model by changing to discrete model and numerical integration, and find a small correction for $\gamma = 1.3$. Second, neither the original nor the modified model appears to fit the data in our data set. Instead of a concave curve as claimed by Levy, we find essentially a straight line. Indeed, if the last two data points of their data set are removed, their result also is consistent with a straight line.

In order to illuminate the apparent inconsistency of our fit with Levy's model, we calculated the histogram of frame-to-frame steps. For bare DNA, the result is shown in Fig. 8(a). A

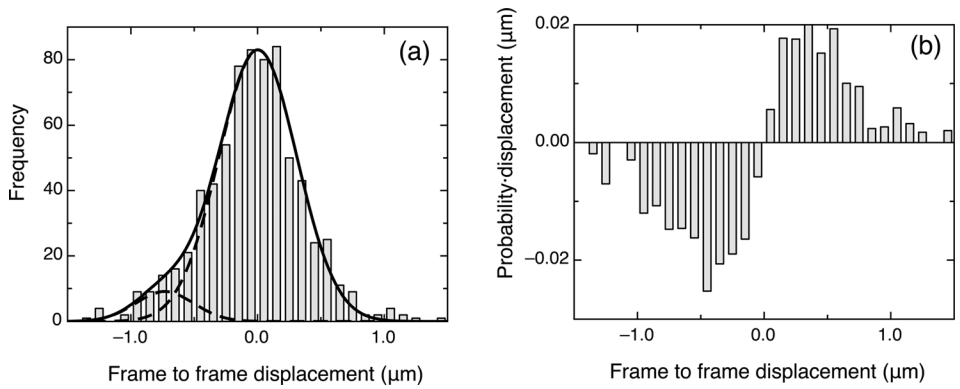

FIG. 8. Statistical properties of folded length for bare DNA. (a) Frame to frame statistics of displacements of folded length. The solid line is the composite fit, while the dashed lines are the individual Gaussians. The fit parameters (with 1 σ error) for the main peak are center position 0.003 ± 0.025 μm, standard deviation 0.308 ± 0.015 μm, number of molecules 208 ± 5. The fit parameters for the weaker feature are center position -0.734 ± 0.118 μm, standard deviation 0.231 ± 0.097 μm, and number of molecules 22.8 ± 4.5. (b) Probabilities in (a) weighted with displacements, i.e., a histogram of the probability-displacement product.

single Gaussian fit (not) shown showed a considerable underfitting in the region of -1.0 to $-0.5\,\mu$m. We thus fitted to two Gaussians, where one Gaussian has mean displacement of approximately 0 with 208 ± 5 counts attributed. A secondary feature emerges at $-0.75\,\mu$m displacement (frames are spaced by 50 ms). However, since only 1/10th of all counts are attributed to the secondary feature (22.8 ± 4.5), the location and width of the feature carry large uncertainties. Upon inspection of the original image data (Fig. 4), we observe that it appears to contain long phases of relatively little change that are interrupted by short periods of rapid shortening of the looped region. Inspection of Levy's data shows the same dynamics. Note that the secondary feature leads to a very large effect on the total movement of the chains as these periods carry a high weight due to the large displacement (Fig. 8(b)).

We speculate that the unrolling does not progress through a continuous process, but rather one that is characterized by starts and stops which is linked to entanglement of the two chains occupying the same channel segment. In particular, the central feature appears to correspond to the relatively stable folded configurations that Chen observed,[72] and we suggest that the importance of the feature in our data is due to the fact that our molecules are 8 times longer than in their publication. We can probe whether the displacement in the histogram is due to random motion, or the effect of a hypothetical two-state motion. To this end, we form the mean over three consecutive displacements, and the re-calculate the histogram. We find that the central peak has narrowed approximately by a factor of $\sqrt{3}$, as expected for thermal fluctuations with a short relaxation time, or errors in fitting. However, the negative displacement feature did not shift significantly, and became even more distinct. Thus, we conclude that steps of rapid unrolling are typically occurring together. We believe that the local rate of unlooping within these should follow Levy's model.

We now turn to the histogram obtained when T4 DNA ligase and ATP are added (Fig. 9(a)). We chose the three-step averaged form since the narrower distribution makes visual comparison easier. We find that upon adding T4 DNA ligase to DNA, the shape and distribution of the central peak does not shift significantly. The secondary feature disappears in the isolated form, but is possibly reflected by a large weight at about $-0.15\,\mu$m in Fig. 9(b). Since the rapid unrolling typical of the "jumps" occurred in irregular intervals, the alignment of the unrolling curves in Fig. 5 does typically "grab onto" the slow creep phases. Thus, the similar shape of the main feature for bare DNA and that bound to T4 DNA ligase leads to a similar numerical measure of relaxation.

Upon addition of ATP to DNA and T4 DNA ligase, the mean displacement of the central peak is considerably reduced, and the peak width apparently is reduced. No secondary feature is discernable. The reduction in mean displacement is directly reflected in the mean unrolling speed in Fig. 5. We believe that the reduction in peak width indicates that DNA segments are not free to move past other segments. Note that the length fluctuations for fully extended DNA molecules in Table I showed no change at the same time.

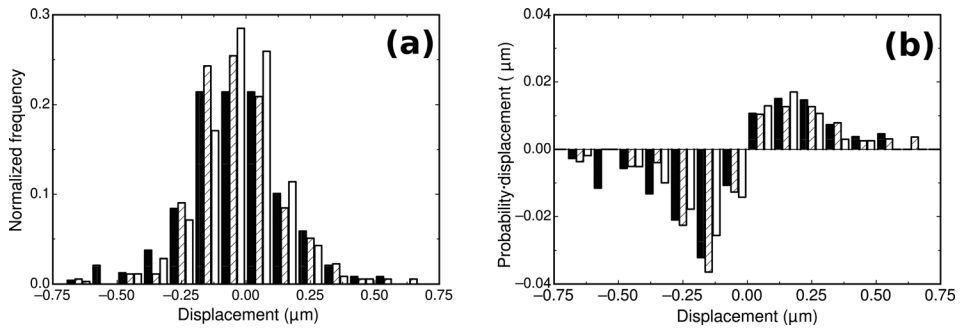

FIG. 9. Histograms of 3-frame averaged displacement of folded length. (a) Histogram showing bare DNA (solid), after addition of T4 ligase (diagonal stripes), and with T4 ligase and ATP (outlined dots). (b) Product of probabilities in (a) and displacement.

We will now attempt to attribute the differing dynamics in the light of the likely biological function of T4 DNA ligase and DNA polymer behavior. Above we have hypothesized that the creeping motion is an effect of mutual entanglement of the two strands occupying the same volume, while the jumps are in an untangled state. Following this hypothesis, we conclude that addition of T4 ligase either reduces the likelihood of disentanglement dramatically, or increases the likelihood of re-entanglement. Both the reduction in persistence length, as well as the reduction in effective polymer width would lead to such an effect, due to the likelihood of entanglement, and the lowering of the effective driving force.

Upon binding of ATP, we anticipate that the interaction between DNA and T4 DNA ligase becomes considerably more specific. The uniform modification of γ has already demonstrated that ligase binds uniformly along the molecule. We thus believe that the significant reduction of the mean displacement in Fig. 9(b) is a testament of increased binding stability of T4 DNA ligase to DNA, and dimerization of T4 DNA ligase molecules on neighboring strands. T4 DNA ligase could potentially slide along the DNA, but we believe that it is likely to stall at intercalating dyes and single-stranded DNA defects induced by oxidative damage during dye bleaching.[73,74] ATP has previously been identified as being necessary for specific binding to single-site defects. Since multiple bound enzymes can act to stabilize the same loop, the ability of ligase oligomers to stabilize folded configuration is a function of both binding constant of ligase and the coverage.

This picture is further solidified by our finding that the majority of DNA-DNA crossings were occupied by T4 DNA ligase in AFM measurements. Based on the dynamic light scattering data, this T4 DNA ligase is likely in not in a monomeric state. Thus, it appears that one T4 DNA ligase is bound to each DNA strand, and the oligomerization drives the coordination of the strands.

We further believe that the DNA-DNA crossings observed in AFM are present before the DNA is deposited on the substrate, and not simply a result of the deposition of a 3-dimensional molecule onto the 2-dimensional substrate. We base this statement on the statistics of molecule entry into nanochannels (Table I). At the pressures used for the majority of experiments, the fraction of DNA molecules entering channels was considerably lower for bare DNA when compared to both samples with T4 DNA ligase. This increase upon ligase binding could be due to a reduction in w and P, but also the formation of a looped structure prior to insertion into the nanochannel. While the first factor doubtlessly plays a role, we have concrete evidence for the second one as well.

For this, we lowered the injection pressure, which resulted in near complete disappearance of folded configurations for bare DNA, while DNA in the presence of T4 DNA ligase still entered with loops. However, the configuration was such that the folded segment trailed the molecule through the channel. That in stark contrast to loops at high driving pressure,[75] and in particular loops in the absence of T4 DNA ligase, where we see almost exclusively folded segments leading the molecule. The only explanation for this asymmetry is the formation of transient loops in solution. Remarkably, this occurs even in the absence of Mg^{2+} (although a small number of Mg^{2+} ions could be remaining from expression of the protein).

V. CONCLUSIONS

We have presented evidence that the physical behavior of nanoconfined DNA is significantly altered in the presence of T4 DNA ligase. In particular, the characteristic stretching of DNA in nanochannels is reduced. We have found evidence of dense binding of protein along the molecule. T4 DNA ligase binding reduced the product of effective DNA width and persistence length by more than a factor of 2, and greatly increased the stability of folded geometries within nanofluidic channels. We hypothesize that bound ligase molecules on neighboring strands can dimerize, and that they in essence stabilize parallel configurations of two DNA strands. We further found evidence for temporary loops in solution that are stabilized by transient ligase-induced links. We believe that such transient protein loops are mobile, and may form an important pathway for the efficient formation of specific large-scale DNA loops.

ACKNOWLEDGMENTS

This work was supported by the National Institutes of Health (National Cancer Institute R21CA132075, National Institutes Child Health and Human Development R21HD065222, National Institute of Environmental Health Sciences R00ES016758). The content is solely the responsibility of the authors and does not necessarily represent the official views of the National Institutes of Health.

[1]S. E. Halford, A. J.Welsh, and M. D. Szczelkun, "Enzyme-mediated DNA looping," Annu. Rev. Biophys. Biomol. Struct. **33**, 1–24 (2004).
[2]R. Schleif, "DNA looping," Annu. Rev. Biochem. **61**, 199–223 (1992).
[3]W. Su, S. Jackson, R. Tjian, and H. Echols, "DNA looping between sites for transcriptional activation: self-association of DNA-bound Sp1," Genes Dev. **5**, 820–826 (1991).
[4]Y. Jiang and P. E. Marszalek, "Atomic force microscopy captures MutS tetramers initiating DNA mismatch repair," EMBO J. **30**, 2881–2893 (2011).
[5]R. M. Stansel, T. de Lange, and J. D. Griffith, "T-loop assembly in vitro involves binding of TRF2 near the 3' telomeric overhang," EMBO J. **20**, 5532–5540 (2001).
[6]S. Adhya, "Multipartite genetic control elements: Communication by DNA loop," Annu. Rev. Genet. **23**, 227–250 (1989).
[7]S. Courbet, S. Gay, N. Arnoult, G. Wronka, M. Anglana, O. Brison, and M. Debatisse, "Replication fork movement sets chromatin loop size and origin choice in mammalian cells," Nature **455**, 557–560 (2008).
[8]E. Lieberman-Aiden *et al*., "Comprehensive mapping of long-range interactions reveals folding principles of the human genome," Science **326**, 289–293 (2009).
[9]N. Naumova, M. Imakaev, G. Fudenberg, Y. Zhan, B. R. Lajoie, L. A. Mirny, and J. Dekker, "Organization of the mitotic chromosome," Science **342**, 948–953 (2013).
[10]L. Cui, I. Murchland, K. E. Shearwin, and I. B. Dodd, "Enhancer-like long-range transcriptional activation by λ CI-mediated DNA looping," Proc. Natl. Acad. Sci. U.S.A. **110**, 2922–2927 (2013).
[11]D. Lewis, P. Le, C. Zurla, L. Finzi, and S. Adhya, "Multilevel autoregulation of λ repressor protein CI by DNA looping *in vitro*," Proc. Natl. Acad. Sci. U.S.A. **108**, 14807–14812 (2011).
[12]J.-F. Allemand, S. Cocco, N. Douarche, and G. Lia, "Loops in DNA: An overview of experimental and theoretical approaches," Eur. Phys. J. E **19**, 293–302 (2006).
[13]E. Alipour and J. F. Marko, "Self-organization of domain structures by DNA-loop-extruding enzymes," Nucl. Acids Res. **40**, 11202–11212 (2012).
[14]C. A. Brackley, S. Taylor, A. Papantonis, P. R. Cook, and D. Marenduzzo, "Nonspecific bridging-induced attraction drives clustering of DNA-binding proteins and genome organization," Proc. Natl. Acad. Sci. U.S.A. **110**, E3605–E3611 (2013).
[15]L. S. Shlyakhtenko, V. N. Potaman, R. R. Sinden, A. A. Gall, and Y. L. Lyubchenko, "Structure and dynamics of three-way DNA junctions: atomic force microscopy studies," Nucl. Acids Res. **28**, 3472–3477 (2000).
[16]Z. Katiliene, E. Katilius, and N. W. Woodbury, "Single molecule detection of DNA looping by NgoMIV restriction endonuclease," Biophys. J. **84**, 4053–4061 (2003).
[17]S. Chatterjee, Y. N. Zhou, S. Roy, and S. Adhya, "Interaction of Gal repressor with inducer and operator: Induction of gal transcription from repressor-bound DNA," Proc. Natl. Acad. Sci. U.S.A. **94**, 2957–2962 (1997).
[18]L. Finzi and J. Gelles, "Measurement of lactose repressor-mediated loop formation and breakdown in single DNA-molecules," Science **267**, 378–380 (1995).
[19]C. Manzo, C. Zurla, D. D. Dunlap, and L. Finzi, "The effect of nonspecific binding of lambda repressor on DNA looping dynamics," Biophys. J. **103**, 1753–1761 (2012).
[20]H. Wang, I. B. Dodd, D. D. Dunlap, K. E. Shearwin, and L. Finzi, "Single molecule analysis of DNA wrapping and looping by a circular 14mer wheel of the bacteriophage 186 CI repressor," Nucl. Acids Res. **41**, 5746–5756 (2013).
[21]S. M. Hamdan, J. J. Loparo, M. Takahashi, C. C. Richardson, and A. M. van Oijen, "Dynamics of DNA replication loops reveal temporal control of lagging-strand synthesis," Nature **457**, 336–339 (2009).
[22]M. Sun, T. Nishino, and J. F. Marko, "The SMC1-SMC3 cohesin heterodimer structures DNA through supercoiling-dependent loop formation," Nucl. Acids Res. **41**, 6149–6160 (2013).
[23]Y.-F. Chen, J. N. Milstein, and J.-C. Meiners, "Protein-mediated DNA loop formation and breakdown in a fluctuating environment," Phys. Rev. Lett. **104**, 258103 (2010).
[24]Z. Hensel, X. Weng, A. C. Lagda, and J. Xiao, "Transcription-factor-mediated DNA looping probed by high-resolution, single-molecule imaging in live *E. coli* cells," PLoS Biol. **11**, e1001591 (2013).
[25]Y. Doksani, J. Y. Wu, T. de Lange, and X. Zhuang, "Super-resolution fluorescence imaging of telomeres reveals TRF2-dependent T-loop formation," Cell **155**, 345–356 (2013).
[26]D. Skoko *et al*., "Barrier-to-autointegration factor (BAF) condenses DNA by looping," Proc. Natl. Acad. Sci. U.S.A. **106**, 16610–16615 (2009).
[27]J. O. Tegenfeldt *et al*., "The dynamics of genomic-length DNA molecules in 100-nm channels," Proc. Natl. Acad. Sci. U.S.A. **101**, 10979–10983 (2004).
[28]D. R. Tree, Y. Wang, and K. D. Dorfman, "Extension of DNA in a nanochannel as a rod-to-coil transition," Phys. Rev. Lett. **110**, 208103 (2013).
[29]W. Reisner, J. Beech, N. Larsen, H. Flyvbjerg, A. Kristensen, and J. O. Tegenfeldt, "Nanoconfinement-enhanced conformational response of single DNA molecules to changes in ionic environment," Phys. Rev. Lett. **99**, 058302 (2007).
[30]D. E. Streng, S. F. Lim, J. Pan, A. Karpusenka, and R. Riehn, "Stretching chromatin through confinement," Lab Chip **9**, 2772–2774 (2009).

[31]C. Zhang, D. Guttula, F. Liu, P. P. Malar, S. Y. Ng, L. Dai, P. S. Doyle, J. A. van Kan, and J. R. C. van der Maarel, "Effect of H-NS on the elongation and compaction of single DNA molecules in a nanospace," Soft Matter **9**, 9593–9601 (2013).
[32]K. Frykholm, M. Alizadehheidari, J. Fritzsche, J. Wigenius, M. Modesti, F. Persson, and F. Westerlund, "Probing physical properties of a DNA-protein complex using nanofluidic channels," Small **10**, 884–887 (2014).
[33]W. Reisner *et al.*, "Statics and dynamics of single DNA molecules confined in nanochannels," Phys. Rev. Lett. **94**, 196101 (2005).
[34]J. H. Carpenter, A. Karpusenko, J. Pan, S. F. Lim, and R. Riehn, "Density fluctuations dispersion relationship for a polymer confined to a nanotube," Appl. Phys. Lett. **98**, 253704 (2011).
[35]A. Karpusenko, J. H. Carpenter, C. Zhou, S. F. Lim, J. Pan, and R. Riehn, "Fluctuation modes of nanoconfined DNA," J. Appl. Phys. **111**, 24701–247018 (2012).
[36]S. L. Levy, J. T. Mannion, J. Cheng, C. H. Reccius, and H. G. Craighead, "Entropic unfolding of DNA molecules in nanofluidic channels," Nano Lett. **8**, 3839–3844 (2008).
[37]R. Metzler, W. Reisner, R. Riehn, R. Austin, J. O. Tegenfeldt, and I. M. Sokolov, "Diffusion mechanisms of localised knots along a polymer," Europhys. Lett. **76**, 696–702 (2006).
[38]D. Shore, J. Langowski, and R. L. Baldwin, "DNA flexibility studied by covalent closure of short fragments into circles," Proc. Natl. Acad. Sci. U.S.A. **78**, 4833–4837 (1981).
[39]D. Shore and R. L. Baldwin, "Energetics of DNA twisting. I. Relation between twist and cyclization probability," J. Mol. Biol. **170**, 957–981 (1983).
[40]J. Shimada and H. Yamakawa, "Ring-closure probabilities for twisted wormlike chains. Application to DNA," Macromolecules **17**, 689–698 (1984).
[41]W. H. Taylor and P. J. Hagerman, "Application of the method of phage T4 DNA ligase-catalyzed ring-closure to the study of DNA structure. II. NaCl-dependence of DNA flexibility and helical repeat," J. Mol. Biol. **212**, 363–376 (1990).
[42]I. R. Lehman, "DNA ligase: structure, mechanism, and function," Science **186**, 790–797 (1974).
[43]H. Kuhn and M. D. Frank-Kamenetskii, "Template-independent ligation of single-stranded DNA by T4 DNA ligase," FEBS J. **272**, 5991–6000 (2005).
[44]S. V. Nilsson and G. Magnusson, "Sealing of gaps in duplex DNA by T4 DNA ligase," Nucl. Acids Res. **10**, 1425–1437 (1982).
[45]D. F. Bogenhagen and K. G. Pinz, "The action of DNA ligase at abasic sites in DNA," J. Biol. Chem. **273**, 7888–7893 (1998).
[46]R. Rossi, A. Montecucco, G. Ciarrocchi, G. Biamonti, and G. Ciarochhi, "Functional characterization of the T4 DNA ligase: A new insight into the mechanism of action," Nucl. Acids Res. **25**, 2106–2113 (1997).
[47]A. V. Cherepanov and S. de Vries, "Dynamic mechanism of nick recognition by DNA ligase," Eur. J. Biochem. **269**, 5993–5999 (2002).
[48]T. E. Cloutier and J. Widom, "Spontaneous sharp bending of double-stranded DNA," Mol. Cell **14**, 355–362 (2004).
[49]Q. Du, C. Smith, N. Shiffeldrim, M. Vologodskaia, and A. Vologodskii, "Cyclization of short DNA fragments and bending fluctuations of the double helix," Proc. Natl. Acad. Sci. U.S.A. **102**, 5397–5402 (2005).
[50]C. Yuan, X. W. Lou, E. Rhoades, H. Chen, and L. A. Archer, "T4 DNA ligase is more than an effective trap of cyclized dsDNA," Nucl. Acids Res. **35**, 5294–5302 (2007).
[51]P. J. Hagerman and V. A. Ramadevi, "Application of the method of phage T4 DNA ligase-catalyzed ring-closure to the study of DNA structure. I. Computational analysis," J. Mol. Biol. **212**, 351–362 (1990).
[52]A. Rosa, N. B. Becker, and R. Everaers, "Looping probabilities in model interphase chromosomes," Biophys. J. **98**, 2410–2419 (2010).
[53]P. H. Von Hippel and O. G. Berg, "Facilitated target location in biological systems," J. Biol. Chem. **264**, 675–678 (1989).
[54]M. Reuter and D. T. F. Dryden, "The kinetics of YOYO-1 intercalation into single molecules of double-stranded DNA," Biochem. Biophys. Res. Commun. **403**, 225–229 (2010).
[55]T. E. Cloutier and J. Widom, "DNA twisting flexibility and the formation of sharply looped protein-DNA complexes," Proc. Natl. Acad. Sci. U.S.A. **102**, 3645–3650 (2005).
[56]R. Riehn, W. Reisner, J. O. Tegenfeldt, Y. M. Wang, C.-K. Tung, S. F. Lim, E. C. Cox, J. Sturm, and R. H. Austin, "Nanochannels for genomic DNA analysis: The long and short of It," in *Integrated Biochips for DNA Analysis*, edited by R. H. Liu and A. P. Lee (Landes Bioscience, Austin, Texas, 2007), pp. 151–186.
[57]R. Riehn, M. C. Lu, Y. M. Wang, S. F. Lim, E. C. Cox, and R. H. Austin, "Restriction mapping in nanofluidic devices," Proc. Natl. Acad. Sci. U.S.A. **102**, 10012–10016 (2005).
[58]P. Kaur *et al.*, "Antibody-unfolding and metastable-state binding in force spectroscopy and recognition imaging," Biophys. J. **100**, 243–250 (2011).
[59]L. Dai, S. Y. Ng, P. S. Doyle, and J. R. C.van der Maarel, "Conformation model of back-folding and looping of a single DNA molecule confined inside a nanochannel," ACS Macro Lett. **1**, 1046–1050 (2012).
[60]F. Persson, P. Utko, W. Reisner, N. B. Larsen, and A. Kristensen, "Confinement spectroscopy: probing single DNA molecules with tapered nanochannels," Nano Lett. **9**, 1382–1385 (2009).
[61]P. G. De Gennes, *Scaling Concepts in Polymer Physics* (Cornell University Press, Ithaca, NY, 1979).
[62]D. W. Schaefer, J. F. Joanny, and P. Pincus, "Dynamics of semiflexible polymers in solution," Macromolecules **13**, 1280–1289 (1980).
[63]Y. Wang, D. R. Tree, and K. D. Dorfman, "Simulation of DNA extension in nanochannels," Macromolecules **44**, 6594–6604 (2011).
[64]F. Persson, F. Westerlund, J. O. Tegenfeldt, and A. Kristensen, "Local conformation of confined DNA studied using emission polarization anisotropy," Small **5**, 190–193 (2009).
[65]C. Zhang, P. G. Shao, J. A. van Kan, and J. R. C. van der Maarel, "Macromolecular crowding induced elongation and compaction of single DNA molecules confined in a nanochannel," Proc. Natl. Acad. Sci. U.S.A. **106**, 16651–16656 (2009).
[66]J. Jones, J. van der Maarel, and P. Doyle, "Effect of nanochannel geometry on DNA structure in the presence of macromolecular crowding agent," Nano Lett. **11**, 5047–5053 (2011).

[67]C. Zhang, Z. Gong, D. Guttula, P. P. Malar, J. A. van Kan, P. S. Doyle, and J. R. C. van der Maarel, "Nanofluidic compaction of DNA by like-charged protein," J. Phys. Chem. B **116**, 3031–3036 (2012).
[68]S. Jun, D. Thirumalai, and B.-Y. Ha, "Compression and stretching of a self-avoiding chain in cylindrical nanopores," Phys. Rev. Lett. **101**, 138101/1–138101/4 (2008).
[69]P. Cifra, "Weak-to-strong confinement transition of semi-flexible macromolecules in slit and in channel," J. Chem. Phys. **136**, 024902 (2012).
[70]P. Cifra and T. Bleha, "Detection of chain backfolding in simulation of DNA in nanofluidic channels," Soft Matter **8**, 9022 (2012).
[71]D. Račko and P. Cifra, "Segregation of semiflexible macromolecules in nanochannel," J. Chem. Phys. **138**, 184904 (2013).
[72]Y.-L. Chen, "Electro-entropic excluded volume effects on DNA looping and relaxation in nanochannels," Biomicrofluidics **7**, 54119 (2013).
[73]B. Akerman and E. Tuite, "Single- and double-strand photocleavage of DNA by YO, YOYO, and TOTO," Nucl. Acids Res. **24**, 1080–1090 (1996).
[74]S. Gurrieri, K. S. Wells, I. D. Johnson, and C. Bustamante, "Direct visualization of individual DNA molecules by fluorescence microscopy: characterization of the factors affecting signal/background and optimization of imaging conditions using YOYO," Anal. Biochem. **249**, 44–53 (1997).
[75]C. H. Reccius, S. M. Stavis, J. T. Mannion, L. P. Walker, and H. G.Craighead, "Conformation, length, and speed measurements of electrodynamically stretched DNA in nanochannels," Biophys. J. **95**, 273–286 (2008).